Enhancement Technique for Aerial Images

Sertan Erkanli
Old Dominion University
Electrical and Computer
Engineering Department Norfolk
VA, USA.
Aeronautics and Space
Technologies Institute, AFA,
Istanbul, Turkey 34807
e-mail: sertanli@yahoo.com

Ahmet Gungor Pakfiliz
Ankara University
Electronics Engineering
Department
Ankara, Turkey 06100
e-mail: agpakfiliz@yahoo.com.tr

Jiang Li
Electrical and Computer
Engineering Department,
Old Dominion University,
Norfolk, VA, USA 23521
e-mail: jli@odu.edu

***Abstract*—Recently, we proposed an enhancement technique for uniformly and non-uniformly illuminated dark images that provides high color accuracy and better balance between the luminance and the contrast in images to improve the visual representations of digital images. In this paper we define an improved version of the proposed algorithm to enhance aerial images in order to reduce the gap between direct observation of a scene and its recorded image.**

I. INTRODUCTION

The human visual system (HVS) perceives colors and detail across a wide range of photometric intensity levels much better than the best recording equipment since HSV is color constant and the perceived color of objects is almost independent of the type of illumination [1-3]. Recorded images are subject to a wide variety of distortions which may result in visual quality degradations. Degradations arises from sensor nonlinearity, optimal defect, the limited dynamic range, that can be captured by cameras, and the turbidity caused by the fog, haze and clouds [4].

Aerial imaging is one of the most common and versatile way of obtaining information from the Earth surface. The images captured form aircraft's, unmanned air vehicle (UAV) or satellites, with operating altitudes ranging from hundreds of meters to hundreds of kilometers. In recent years, increased of UAV's aerial images has been increased use as a tool for various military and non-military applications. These UAV's have many advantages such over conventional aircraft that they cost far less to operate, they can be launched in rugged terrain and they do not put human lives in danger when used. These advantages make the use of camera- equipped UAV's feasible [5, 7].

The flying higher and using wide-angle lenses increase the field of view and hence the search area coverage, but it also obviously reduces the resolution. The limited dynamic range of camera, the poor weather conditions, which are introducing artifacts into image, and signal to noise ratio due to the thermal characteristics of device electronics, results in aerial images with locally poor contrast. The recorded images not easily observable by HSV need to undergo some preprocessing such enhancement, restoration, deblurring in order to be usually followed by feature detection, used in various applications such as object detection, tracking and classification [8-10].

The idea behind enhancement techniques aim to match the recorded image to the observed image in order to adequately represent the directly observed scene with bringing out details in images that are otherwise too dim to be perceived either due to insufficient brightness or insufficient contrast. A large number of image enhancement methods have been developed, like log transformations, power law transformations, piecewise-linear transformations and histogram equalization. However these enhancement techniques are based on *global* processing which results in a single mapping between the input and the output intensity space. Other image enhancement techniques are *local* in nature, i.e., the output value depends not only on the input pixel value but also on pixel values in the neighborhood of pixel. These techniques are able to improve local contrast under various illumination conditions [11-22].

Recently we have developed enhancement technique for uniformly and non-uniformly illuminated dark images (ETNUD) and wavelet based enhancement technique for uniformly and non-uniformly illuminated dark images (WBNUDE) that provide high color accuracy and better balance between the luminance and contrast in images to improve the visual representations of digital images [3-4]. In this paper, we describe modified ETNUD algorithm (METNUD), used in candidate in aerial imagery applications, providing dynamic range compression (DRC) preserving the local contrast and tonal rendition: The details of the new algorithm are given in Section II. Section III describes experimental results and compares our results with other techniques for aerial image enhancement. Finally in Section IV we present our conclusions, and discuss the future direction for this research.

II. ALGORITHM

The proposed modified ETNUD algorithm is composed of three stages. The major innovation in modified ETNUD algorithm is in the selection of the transformation parameters for DRC, and contrast enhancement parameters. The following sections describe the selection mechanisms.

A. Selection of transformation parameters for DRC

The intensity I of the color image I_c can be determined by

$$I(m,n) = 0.2989r(m,n) + 0.587g(m,n) + 0.114b(m,n) \quad (1)$$

where *r*, *g*, *b* are the red, green, and blue components of I_c respectively, and *m* and *n* are the row and column pixel locations respectively. Assuming I to be 8-bits per pixel, I_n is the normalized version of I, such that [2,3]

$$I_n(m,n) = I(m,n)/255 \tag{2}$$

Using linear input-output intensity relationships typically does not produce a good visual representation compared with direct viewing of the scene [18]. Therefore, we use a nonlinear transformation for DRC which is based on some information extracted from the image histogram. To achieve this, we subdivide the histogram of the intensity images into four ranges: r_1 =0–63, r_2= 64–127, r_3 = 128–191 and r_4 = 192–255. I_n is mapped to I_n^{drc} using the following:

$$I_n^{drc} = \begin{cases} (I_n)^x + \alpha & 0 < x < 1 \\ (0.5 + (0.5 I_n)^x) + \alpha & x \geq 1 \end{cases} \tag{3}$$

The first mapping pulls out the details in the dark regions, and the second suppresses the bright overshoots. The value of x is given by

$$x = \begin{cases} 0.2, & if \quad (f(r_1 + r_2) \geq f(r_3 + r_4)) \ \Lambda \ (f(r_1) \geq f(r_2)) \\ 0.5, & if \quad (f(r_1 + r_2) \geq f(r_3 + r_4)) \ \Lambda \ (f(r_1) < f(r_2)) \\ 3.0, & if \quad (f(r_1 + r_2) < f(r_3 + r_4)) \ \Lambda \ (f(r_3) \geq f(r_4)) \\ 5.0, & if \quad (f(r_1 + r_2) < f(r_3 + r_4)) \ \Lambda \ (f(r_3) \geq f(r_4)) \end{cases} \tag{4}$$

where $f(a)$ refers to number of pixels between the range (a), $f(a_1 + a_2) = f(a_1) + f(a_2)$, and Λ is the logical AND operator. α is the offset parameter, helping to adjust the brightness of image. The curves for the two ranges of *x* are shown in Figures 1 and 2. The determination of the *x* values and their association with the range-relationships as given in Equation 4 was done experimentally using a large number of aerial images and *x* value can be also determined manually [2,3].

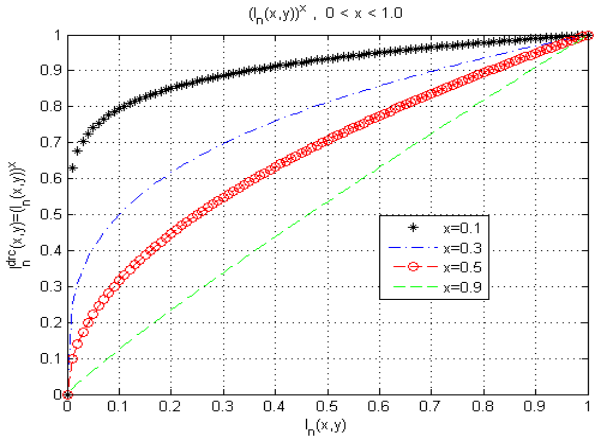

Figure 1. I_n^{drc} for different ranges r_i.

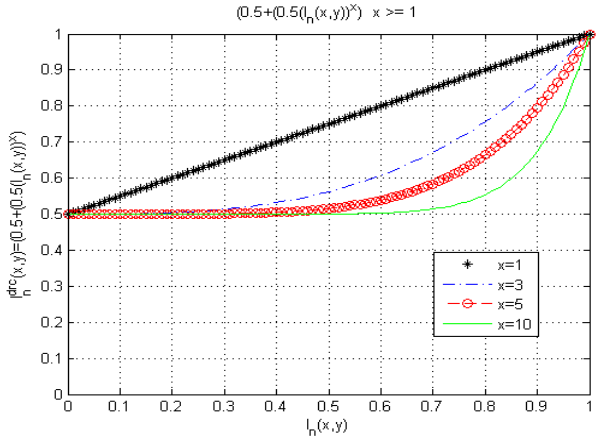

Figure 2. I_n^{drc} for different ranges r_i.

The second transfer function is used for mapping I_n^{drc} to A_{en}^{drc} using the following process: First, I_n^{drc} is mapped to $T(m,n)$ using:

$$T(m,n) = \log \frac{I_n^{drc}(m,n) - \min(I_n^{drc}(m,n)) - 1}{\max(I_n^{drc}(m,n)) + 1 - I_n^{drc}(m,n)} \tag{5}$$

Then $T(m,n)$ is normalized:

$$T_n(m,n) = \frac{T(m,n) - \min(T(m,n))}{\max(T(m,n)) - \min(T(m,n))} \tag{6}$$

$T_n(m,n)$ is mapped to A_{en}^{drc}, the new enhanced approximation coefficients, using the following equation:

$$A_{en}^{drc} = (T_n(m,n)(\alpha - \beta) + \beta)^r$$
$$\alpha = \max(I_n^{drc}) \quad \beta = \min(I_n^{drc}) \tag{7}$$

where *r* is the curvature parameter for adjusting the shape of the transfer function. With this transformation which is based on some information extracted from the image histogram, we can pull out the details in the dark regions while suppressing the bright overshoots. The value of *r* is given by

$$r = \begin{cases} 1.04, & if (f(r_1 + r_2) \geq f(r_3 + r_4)) \ \wedge \ (f(r_1) \geq f(r_2)) \\ 1.02, & if (f(r_1 + r_2) \geq f(r_3 + r_4)) \ \wedge \ (f(r_1) < f(r_2)) \\ 0.98, & if (f(r_1 + r_2) < f(r_3 + r_4)) \ \wedge \ (f(r_3) \geq f(r_4)) \\ 0.96, & if (f(r_1 + r_2) < f(r_3 + r_4)) \ \wedge \ (f(r_3) < f(r_4)) \end{cases} \tag{8}$$

The curves for the Equation 8 are shown in Figure 3. The determination of the *r* values and their association with the range-relationships as given in Equation 8 was done also experimentally using a large number of aerial images and *r* value can be also determined manually.

The DRC mapping of the intensity image performs a visually dramatic transformation. However, it tends to have poor contrast, so a local, pixel dependent contrast enhancement method with new contrast enhancement parameters is used to improve the contrast.

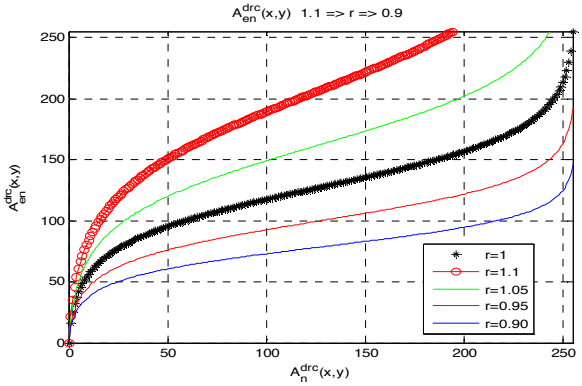

Figure 3 A_{en}^{drc} for a different value of *r*.

B Selection of surround parameter and color restoration

The local contrast enhancement is carried out as follows: The luminance information of surrounding pixels is obtained by using 2D discrete spatial convolution with a Gaussian kernel, *G(m,n)* defined as:

$$G(m,n) = K\exp\left(-\frac{m^2+n^2}{\sigma_s^2}\right) \tag{9}$$

where σ_s is the surround space constant equal to the standard deviation of *G(m,n),* and *K* is determined under the constraint that $\sum_{m,n} G(m,n) = 1$. The center-surround contrast enhancement is defined as:

$$A_{enh}(m,n) = 255A_{enh}^{drc}(m,n)^{E(m,n)} \tag{10}$$

where, *E(m, n)* is given by

$$E(m,n) = \left[\frac{A_{filt}(m,n)}{A(m,n)}\right]^S \tag{11}$$

where

$$A_{filt}(m,n) = A(m,n) * G(m,n) \tag{12}$$

'*' is the convolution operator, and *S* is the adaptive contrast enhancement parameter. *S* is related to the global standard deviation, σ, of the input intensity image, $I(m,n)$ by

$$S = \begin{cases} 5 & for \quad \sigma \le 7 \\ 3 & for \quad 7 < \sigma \le 20 \\ 1 & for \quad \sigma \ge 20 \end{cases} \tag{13}$$

σ is the contrast—standard deviation—of the original intensity image. If $\sigma < 7$, the image has poor contrast and the contrast of the image will be increased. If $\sigma \ge 20$, the image has sufficient contrast and the contrast will not be changed. Finally, the enhanced image can be obtained by linear color restoration based on chromatic information contained in the original image as:

$$S_j(x,y) = A_{enh}(x,y)\frac{I_j(x,y)}{I(x,y)}\lambda_j \tag{14}$$

where $j \in \{r,g,b\}$ represents the RGB spectral band and λ_j is a parameter which adjusts the color hue [2,3].

III. EVALUATION CRITERIA

In this paper, following evaluation criteria is used.

A. A metric

There are some metrics such as brightness and contrast to characterize an image. Another such metric is sharpness. Sharpness is directly proportional to the high-frequency content of an image. So we can define a new metric as [2,3]

$$S = \sqrt{\|h \otimes I\|^2} = \sqrt{\sum_{v_1=0}^{M_1-1}\sum_{v_2=0}^{M_2-1}\left|\hat{h}[v_1,v_2]\hat{I}[v_1,v_2]\right|} \tag{15}$$

where h is a high-pass filter, periodic with period $M_1 x M_2$ and $\hat{h}$ is its direct Discrete Fourier Transform (DFT). I is also DFT of Image *I*. The role of $\hat{h}$ (or *h*) is to weight the energy at the high frequencies relative to the low frequencies, thereby emphasizing the contribution of the high frequencies to *S*. The larger value of *S*, the greater sharpness of *I* and conversely.

Equation 15 defines how the sharpness should be computed and defined as

$$\hat{h}[v_1,v_2] = 1 - \exp\left(-\frac{v_1^2+v_2^2}{\sigma^2}\right) \tag{16}$$

where σ is the parameter at which the attenuation coefficient $= 1.0 - e^{-1} \approx 2/3$. A smaller value of σ implies that fewer frequencies are attenuated and vice versa. We have used in this paper as σ =0.15.

B. Image Quality Assessment

The overall quality of images can be measured by using the brightness μ, contrast σ and sharpness *S*, where brightness and contrast are assumed to be the mean and the standard deviation. However, instead of using global statistics, regional statistics is used. In order to do this [2]:

1) Divide the $M_1 x M_2$ image *I* into $(M_1/10)x(M_2/10)$ non-overlapping blocks, $I_i, i=1,\ldots,100$, such that $I \approx \cup_{i=1}^{N} I_i$, (Total Number of Regions are 100).

2) For each block compute the measures, μ, σ and *S*,

3) Classify the block as either GOOD or POOR based on the computed measure (will be discussed with the following).

4) Classify the image as a whole as GOOD or POOR based upon the classification of regions (will be discussed with the following).

The following criterions are used for brightness, contrast and sharpness [16]:

1) Let μ_n be normalized brightness parameter, such that

$$\mu_n = \begin{cases} \mu/255 & \mu < 154 \\ 1-\mu/255 & otherwise \end{cases} \quad (17)$$

A region is considered to have sufficient brightness when $0.4 \le \mu_n \le 0.6$.

2) Let σ_n be normalized contrast parameter, such that

$$\sigma_n = \begin{cases} \sigma/128 & \mu \le 64 \\ 1-\sigma/128 & otherwise \end{cases} \quad (18)$$

A region is considered to have sufficient contrast when $0.25 \le \sigma_n \le 0.5$. When $\sigma_n < 0.25$, the region has poor contrast, and when $\sigma_n > 0.5$, the region has too much contrast.

3) Let S_n be normalized sharpness parameter, such that $S_n = min(2.0, S/100)$. When $S_n > 0.8$, the region has sufficient sharpness. The Image Quality is evaluated using by

$$Q = 0.5\mu_n + \sigma_n + 0.1S_n \quad (19)$$

where $0 < Q < 1.0$ is the quality factor. A region is classified as good when $Q > 0.55$, and poor when $\sigma_n \le 0.5$. An image is classified as GOOD when the total number of regions classified as GOOD, $N_G > 0.6N$.

IV. EXPERIMENTAL RESULT

The image samples for METNUD were selected to be as diverse as possible so that the result would be as general as possible. We used MATLAB for AINDANE and IRME that was developed by the authors. MSRCR enhancement and histogram equalization were done with commercial software, PhotoFlair. From our own visual experience, we make the following statements about the proposed algorithm:

1) In the Luminance enhancement part it has been shown that METNUD works well for dark, foggy and hazy images and the technique adjusts itself to the image (Figure 4).

2) In the contrast enhancement part it is clear that unseen or barely seen features of low contrast images are made visible (Figure 4).

3) The results in Fig.4 show modified algorithm works well for images captured from diverse angle conditions. The METNUD algorithm gives good result (in Table 1.)

4) In Figure 5 histogram equalization does not provide good visual enhancement. IRME and MSRCR bring out the details in the dark but have some enhancement in the bright regions which can be considered objectionable. AINDANE does not bring out the finer details of the images and seem blurry. The METNUD provides better visibility enhancement the best sharpness can be adjusted by the α parameter in Equation 3.

TABLE I. The results of Evaluation Criteria

Figure 3	ORIGINAL IMAGE NUMBER OF REGIONS GOOD	POOR	ETNUD NUMBER OF REGIONS GOOD	POOR
TOP ROW IMAGE	95	5	99	1
SECOND ROW IMAGE	96	4	100	-
THIRD ROW IMAGE	92	8	99	1
LAST ROW IMAGE	100	-	100	-

V. CONCLUSION

METNUD image enhancement algorithm provides high color accuracy and better balance between the luminance and contrast in image has been developed to improve the visual representations of digital images. The results show strong robustness, improved visibility and high image quality. For further research, the algorithm is going to be implemented in the discrete wavelet domain for reducing the processing time.

REFERENCES

[1] G.A. Woodel, D. J. Jobson, Z. Rahman, and Glenn Hines "Enhancement of imagery in poor conditions," Sensors, and Command, Control, Communications, and Intelligence (C3I) Technologies for Homeland Security and Homeland Defense IV, Proc. SPIE 5778, 2005.

[2] S.Erkanli, Z.Rahman, "Enhancement Technique for Uniformly and Non-Uniformly Illuminated Dark Images," Intelligent Systems Design and Applications (ISDA), 2010 10th International Conference, pp.850-854, 2010.

[3] S.Erkanli, Z.Rahman, "Wavelet Based Enhancement Technique for Uniformly and Non-Uniformly Illuminated Dark Images," Intelligent Systems Design and Applications (ISDA), 2010 10th International Conference, pp.855-859, 2010.

[4] T. A. Mahmoud, "Enhancement Of Aerial Images Using Threshold Decomposition Adaptive Morphological Filter," Image Processing (ICIP), 2009 16th IEEE International Conference, pp. 3121-3124, 2009.

[5] Y. Shen, S.K. Jakkula, “Aerial Image Enhancement Based on Estimation Of Atmospheric Effects," in Applications of Digital Image Processing XIX, A. G. Tescher, ed., Proc. SPIE 2847, 1996.

[6] N. D. Rasmussen, D. R. Thorton, B. S. Morse, “Enhancement of Unusual Color in Aerial Video Sequences for Assisting Wilderness Search and Rescue," Image Processing, ICIP, pp. 1356-1359, 2008.

[7] Y. Chen, Y. Ho, C. Wu, C. Lai, “Aerial Image Clustering using Genetic Algorithm," International Conference on Computational Intelligence for Measurement Systems and Applications, pp. 42-45, 2009.

[8] A. Mansoor, Z. Khan, A. Khan, “An Application of Fuzzy Morphologhy for Enhancement of Aerial Images," International Conference on Advances in Space Technologies, pp. 143-148, 2008.

[9] D. J. Jobson, Z. Rahman, G. A. Woodell, G. D. Hines, A Comparison of Visual Statistics for the Image Enhancement of FORESITE Aerial Images with Those of Major Image Classes Visual Information Processing XV, Proc. SPIE 6246, 2006.

[10] G. A. Woodell, D. J. Jobson, Z. Rahman, G. D. Hines, Advanced Image Processing of Aerial Imagery Visual Information Processing XV, Proc. SPIE 6246, 2006.

[11] J. B. Zimmerman, S. B. Cousins, K. M. Hartzell, M. E. Frisse, and M. G. Kahn, “A psychophysical comparison of two methods for adaptive histogram equalization,” Journal of Digital Imaging, vol. 2, pp.: 82-91, 1989.

[12] S. M. Pizer and E. P. Amburn, “Adaptive histogram equalization and its variations,” Computer Vision, Graphics, and Image Processing, vol. 39, pp.:355-368, 1987.

[13] E. Land and J. McCann, “Lightness and Retinex theory,” Journal of the Optical Society of America, vol. 61, pp.: 1-11, 1971.

[14] A. Hurlbert, “Formal Connections between Lightness Algorithms”, Journal of the Optical Society of America, vol. 3, No 10 pp.: 1684-1693, 1986.

[15] E. Land, “An alternative technique for the computation of the designator in the Retinex theory of color vision,” Proc. of the NationalAcademy of Science USA, vol. 83, pp.: 2078-3080, 1986.

[16] D. J. Jobson, Z. Rahman and G.A. Woodell, “Properties and performance of a center/surround retinex,” IEEE Transactions on Image Processing: Special Issue on Color Processing, No. 6, pp.:451- 462, 1997.

[17] Z. Rahman, D. J. Jobson, and G. A. Woodell, “Multiscale retinex for color image enhancement,” Proc. IEEE International. Conference. on Image Processing, 1996.

[18] D. J. Jobson, Z. Rahman, and G. A. Woodell, “A multi-scale retinex for bridging the gap between color images and the human observation of scenes,” IEEE Transactions on Image Processing, Vol. 6, pp.:965-976, 1997.

[19] Z. Rahman, D. J. Jobson, and G. A. Woodell, “Retinex Processing for Automatic Image Enhancement", Journal of Electronic Imaging, 2004.

[20] L. Tao and K. V. Asari, “An adaptive and integrated neighborhood dependent approach for nonlinear enhancement of color images,” SPIE Journal of Electronic Imaging, Vol. 14, No. 4, ,pp.: 1.1-1.14. 2005.

[21] L. Tao, R. C. Tompkins, and K. V. Asari, “An illuminance-reflectance model for nonlinear enhancement of video stream for homeland security applications,” IEEE International Workshop on Applied Imagery and Pattern Recognition, AIPR - 2005, Washington DC, October 19 - 21, 2005.

[22] K. V. Asari, E. Oguslu, and S. Arigela, “Nonlinear enhancement of extremely high contrast images for visibility improvement,” Lecture Notes in Computer Science, Proc. of the 5th Indian Conference on Computer Vision, Graphics and Image Processing - ICVGIP 2006: vol.4338, pp.:240-251, 2006.

Figure4. The results: Left Column: Original Images, Right Columns: Enhanced Images (METNUD).

Figure 5. Comparisons: (top-left) Original; (top-right) Histogram equalization; (middle-left) IRME; (middle-right) MSR; (bottom-left) AINDANE; (bottom-right) METNUD.